

FRACTAL NATURE OF ACICULAR FERRITE, AND FINE PRECIPITATION IN MEDIUM CARBON MICRO-ALLOYED FORGING STEELS.

R. VILLEGAS⁽¹⁾, A. REDJAIMIA⁽¹⁾, M. CONFENTE⁽²⁾, M. T. PERROT-SIMONETTA⁽²⁾

⁽¹⁾Laboratoire de Science et Génie des Surfaces, Ecole de Mines de Nancy, Parc de Saurupt, 54042 Nancy Cedex, France

⁽²⁾ MITTAL STEEL EUROPE R&D Centre, CRIE BP 140 57360, Amn ville, France

Abstract:

Acicular ferrite (AF) is a highly sub-structured, non-equiaxed ferrite formed upon continuous cooling or isothermally by a mixed diffusion and shear mode of transformation. Unlike bainite which initiates at austenite grain boundaries forming sheaves of parallel plates, the AF nucleates on non-metallic inclusions and allotriomorphic ferrite which decorates the austenitic grain boundaries. Subsequently, the plates grow auto-catalytically producing a chaotic interlocked arrangement. To help understanding this particular space disposition a fractal analysis has been conducted on AF obtained on medium-carbon micro-alloyed steels with variable vanadium contents cooled at different rates. Fractal parameters have been obtained by applying a 2d box-counting method to SEM digital images.

Second phase precipitation and its links with the AF are also often studied. Potentialities of some non-metallic inclusions on AF nucleation are well known. Though, mechanisms involved are unclear and some times the hypotheses proposed to explain them seem contradictories. In the present work, a finer precipitation phenomenon has been considered. An interphase precipitation inside the AF plates has been evidenced and analysed with the help of transmission electron microscopy (TEM).

Key words: acicular ferrite, medium carbon forging steels, micro-alloyed steels, fractal morphology, interphase precipitation.

INTRODUCTION

Bainitic microstructures have been prevailed as main alternatives to ferrite-pearlite ones in structural and forging steels. The excellent mechanical properties obtained with similar production paths and no additional heat treatments explain the great interest granted to these steels from the cost-effectiveness point of view [1, 2]. Fine-grained microstructures composed of a mixed allotriomorphic ferrite and bainite obtained by controlled continuous cooling transformation (CCT) have proved increased yield strength and good toughness in pipelines and plates steels. Though, another alternative microstructure, the acicular ferrite (AF), has also become of special interest for some of the same applications bainite does [6-12].

AF has been observed and studied since decades in heat affected zones (HAZ) in welded low and ultra-low carbon micro-alloyed steels. AF is a highly sub-structured, non-equiaxed ferrite formed upon continuous cooling by a mixed diffusion and shear mode of transformation that begins at a temperature slightly higher than transformation temperature range of upper bainite. Its fine effective grain size, high angle grain boundaries and dislocation density are known to be at the origin of mechanical properties improvement, specially strength and toughness [2, 3, 4, and 5]. Even when AF and bainite share the same transformation regions in CCT diagrams

there is a main observable difference between upper bainite and acicular ferrite. In upper bainite ferrite initiates at austenite grain boundaries forming sheaves of parallel plates with the same or almost the same crystallographic orientation, whereas in AF we found a rather chaotic interlocked arrangement of ferrite plates (Fig.°1.). Some authors state that acicular ferrite is actually nothing but intragranular grown up bainite nucleated at non metallic inclusions [2, 3, 12, 13]. Most of the time AF is also distinguished from bainite in that it has a limited amount of carbon (C) available, there is thus only a small amount of carbide inside it.

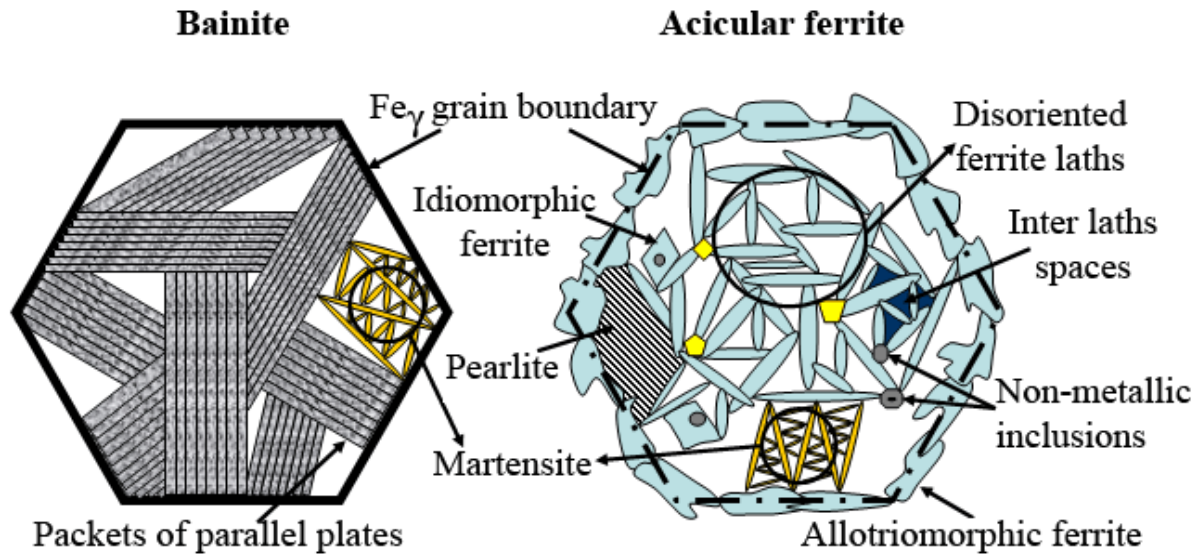


Figure1. Morphological features of bainite and acicular ferrite formation inside Fe_{γ} grain.

Bainite and AF arise from competitive transformation of austenite decompositions products in continuous cooling conditions. Factors as austenite grain size, concentration and nature of non-metallic inclusions and previous nucleation of allotriomorphic ferrite at the former austenite grain boundaries, which inhibits the bainite formation, determine the AF rate in final microstructure composition. These factors are directly affected by chemical composition, austenitisation conditions and cooling rates. In order to optimise parameters mentioned above to obtain maximum AF rates in CCT conditions three vanadium (V) micro-alloyed forging steel formulations were prepared and its microstructures previously analysed by different microscopy techniques [14].

Fractal geometry proposed by Mandelbrot has radically changed the approach of nature description. Mandelbrot [15] and Hornbogen [16] early reported the fractal nature of some microstructures in metals. Since then fractal analysis has become an alternative in describing some microstructures from both qualitative and quantitative point of view [17, 18]. These microstructures show a fractal nature in a certain scale range [19-22]. In the present work fractal analysis of volume filling and space disposition of AF plates have been made. The fractal dimension has been obtained by applying a two dimensional box-counting method to SEM digital images. A simple model of self similar nucleation of AF plates is also proposed.

Another interesting facet often approached is second phase precipitation and its relation to acicular ferrite development. A lot have been revealed about the potentialities of different non metallic inclusions on assisting AF nucleation. Though, the real mechanism behind those potentialities remains unclear and several contradictories hypothesis have been enounced to explain it. A finer inter-phase precipitation has been evidenced and analysed in this work, with transmission electron microscopy (TEM), inside both proeutectoid ferrite and AF plates.

MATERIALS AND METHODS

Microstructures of three medium carbon micro-alloyed steels, FA1, FA2 and FA3 have been previously studied in continuous cooling conditions [14]. Major elements concentrations in chemical composition of steels are presented in Table I.

Table I. Chemical composition (mass-%)

C	Si	Mn	P	S	N	Cu	V	Ti
0.3 — 0.4	0.3 — 0.6	1.2 — 1.6	< 0.02	< 0.04	< 0.2	< 0.2	0.15 — 0.20	< 0.015

Cylindrical samples of $\phi 6.0^{\circ}\text{mm} \times 10.0^{\circ}\text{mm}$ were continuous cooled in a BHR 805 dilatometer at cooling rates of 0.5, 1.0 and 2.5 $^{\circ}\text{C/s}$. To establish the self similarity of AF plates at early stages of formation a particular cooling cycle was performed consisting of continuous cooling at 2.0 $^{\circ}\text{C/s}$ from 1200 $^{\circ}\text{C}$ to 500 $^{\circ}\text{C}$ plus 10.0 s hold at 500 $^{\circ}\text{C}$ before water quenching. Samples were sectioned and analysed in the bulk. Metallographic observations were made after mechanical polishing to 1.0 μm diamond paste and etching with 2 % Nital for optical microscopy (OM) observation and DINO for SEM. For TEM preparation disks of 0.5 mm thick were cut from cylindrical samples, mechanically grinded and mirror polished to 20-30 μm thickness and finally twin jet thinned in a 5% perchloric acid, 15% glycerol, 80% methanol electrolytic bath.

OM was made on a VANOX AHMT3 Olympus apparatus. SEM observations were made in a Philips XL30 SFEG scanning electron microscope, in backscattering secondary electron mode (BSE). A Philips CM200 was used for TEM observations.

Fractal parameters have been obtained applying a bi-dimensional box-counting method to SEM images. Area fraction analysis was made with the help of Aphelion 3.0 software over digital acquired and pre-treated images.

RESULTS AND DISCUSSION

Fractal analysis

Fractal structures are formed by of *ad infinitum* iteration successive generations of geometrically self similar units. In fact, this is true only in a limited physical scale range. It depends on the extents of the latter whether or not the application of more than one microscopic method is needed to make the fractal analysis. Figure 2 highlights the fractal like aspect of AF observed at TEM.

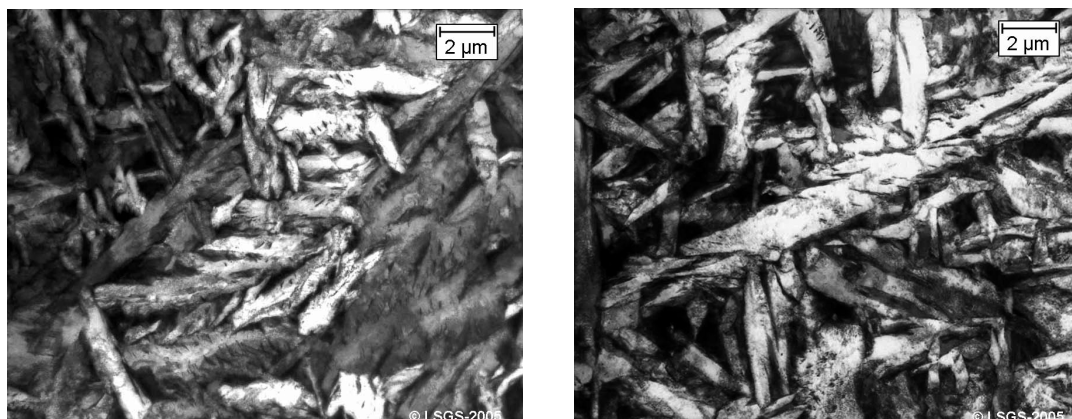


Figure 2. Fractal like aspect of AF at TEM observations.

Two steps are necessary in metallographic fractal analysis: to establish the self-similarity of the structure and to determine the fractal dimension [16]. Fractal microstructures must fill two conditions [19]: (i) more than $x^{\circ} \ddagger^{\circ} 3$ distinguishable self similar fragmentations (generations of AF plates in the present case); (ii) a constant fractal dimension $D >^{\circ} d$ (d : topological dimension) and a self-similarity established for a range of more than one order of magnitude. For practical purposes optical and SEM images were chosen to establish self similarity and SEM digital images to determine the fractal dimension D [22].

The observation of early stages of transformation clearly shows more than three autocatalytic generations of AF. Yang and Bhadeshia found that adjacent plates of AF presented a tendency to form similar orientation in space. They conclude that this may arise because during sympathetic nucleation the formation of plates with approximately the same orientation may be kinetically favoured [5]. Figure 3 shows how apparent angles between plates of successive generations could be approximately the same.

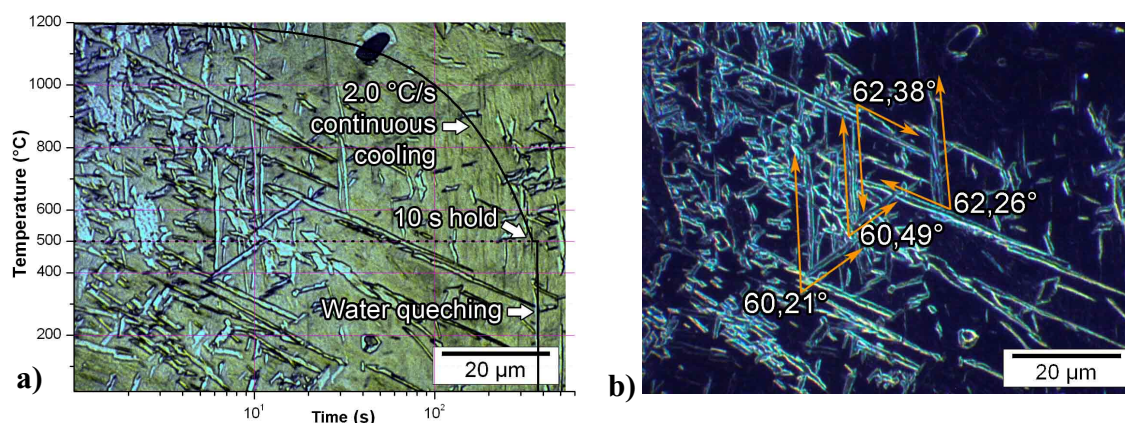


Figure 3. a) Successive generations of autocatalytic AF plates observed at early stages. b) Apparent angles between plates of successive generations, dark field optical image.

Considering the needle like shape of AF plates the aspect ratio was preferred as criterion to find the similarity degree between successive generations. Figure 4 a) shows a typical SEM image used in AF plates aspect ratio estimation. The mean aspect ratio was found to be 1.2 for nearly hundred plates analysed. The histogram of aspect ratio distribution is showed in Figure 4 b) as well as the relation between aspect ratio and length of the plates.

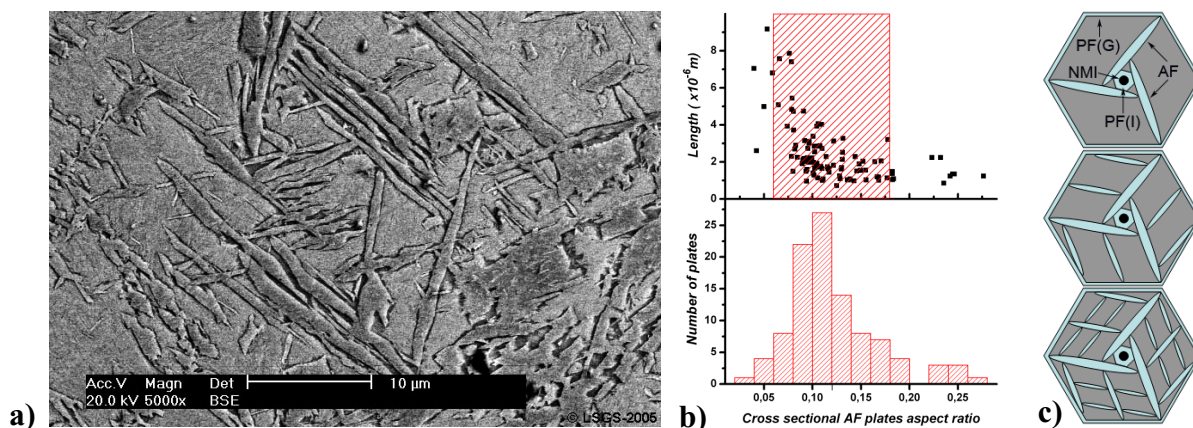


Figure 4. a) SEM image of AF plates early stages. b) AF plates aspect ratio histogram and aspect ratio vs. length plot. c) Simple schematisation of fractal autocatalytic AF. PF(G): allotriomorphic ferrite, NMI: non-metallic inclusions, PF(I): idiomorphic ferrite, AF: AF.

The farthest values from the mean are found to be at both extremes of lengths range. This can be explained by stereological reasons for the smallest plates. In fact a number of plates are certainly oriented in a near normal direction to the section observed. For bigger length plates the aspect ratio is probably influenced by the enlargement of ferrite in time. Nevertheless we can affirm that an acceptable degree of self-similarity exists all along successive generations. Figure 4 c) shows a simple schematisation of fractal autocatalytic AF as it could be for medium carbon micro-alloyed steels. In fact at studied cooling rate non metallic inclusions susceptible of act as nucleation sites were systematically covered of idiomorphic ferrite, and AF plates seems to nucleate from the latter. Austenite grain boundaries were also completely decorated by allotriomorphic ferrite.

The application of the bi-dimensional box-counting method to SEM images to analyse the space filling by AF plates demonstrate the existence of a not integer dimension bigger than topological dimension in a scale range between [0.5°—12.0° m] (Figure 5).

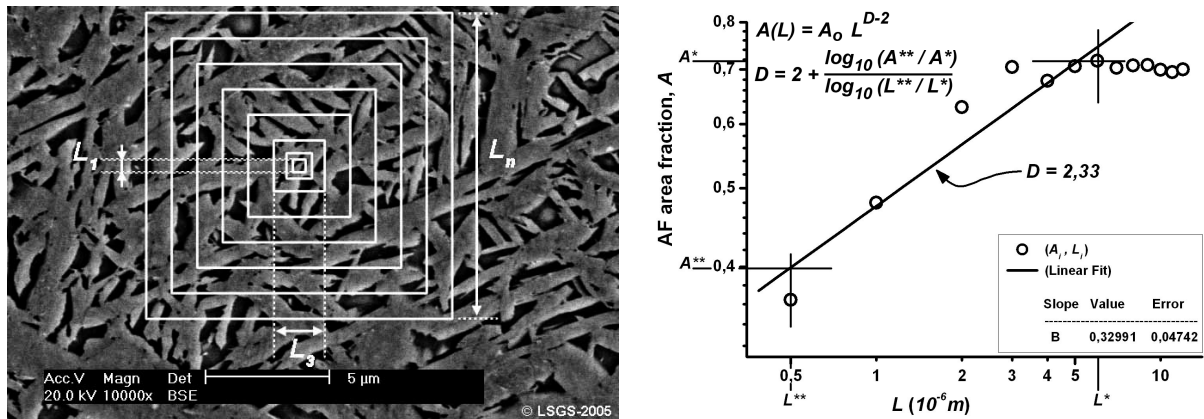


Figure 5. Box-counting method applied to AF microstructure for 2.0 °C/s cooling rate. a) SEM image with 2-dimensional boxes, b) log-log plot of AF area fraction vs. box size.

Averaged values of fractal dimension D and fractal scale range limits L^{**} and L^* for AF in microstructures obtained by continuous at 0.5, 1.0 and 2.0 °C/s cooling rates are showed in Table II. The box-counting method was applied three times for every SEM image analysed varying the boxes centre every time.

Table II. Box-counting method analysis results.

Cooling rate	0.5 °C/s	1.0 °C/s	2.0 °C/s	
Fractal Dimension, D	2.41°—°0.06	2.14°—°0.03	2.11°—°0.02	2.31°—°0.01
Fractal scale range °[L^{**} °—° L^*](m)	[0.5°—°6.0]	[6.0°—°12.0]	[2.0°—°12.0]	[0.5°—°6.0]

For 0.5 °C/s cooling rate a multi fractal character was found with two distinct scale ranges and two different fractal dimensions.

A first step in establishing a possible correlation between fractal parameters and mechanical properties was envisaged. Though, it must be said that a correlation between fractal dimension and mechanical properties of materials does not necessarily exist when properties are influenced also by non-geometrical factors [18].

Hardness Vickers test were performed within regions occupied exclusively by AF (Figure 6 a). A weight charge of 50 g was settled as the best regarding the reproducibility of tests. Results were confronted to fractal parameters. Not visible correlation between Vickers hardness and fractal dimension was found. Whereas simultaneous log-log correlation of cooling rates with inferior limits of fractal scale range, L^{**} , and Vickers hardness shows an inverse relation (Figure 6 b). Further mechanical test are undertaken.

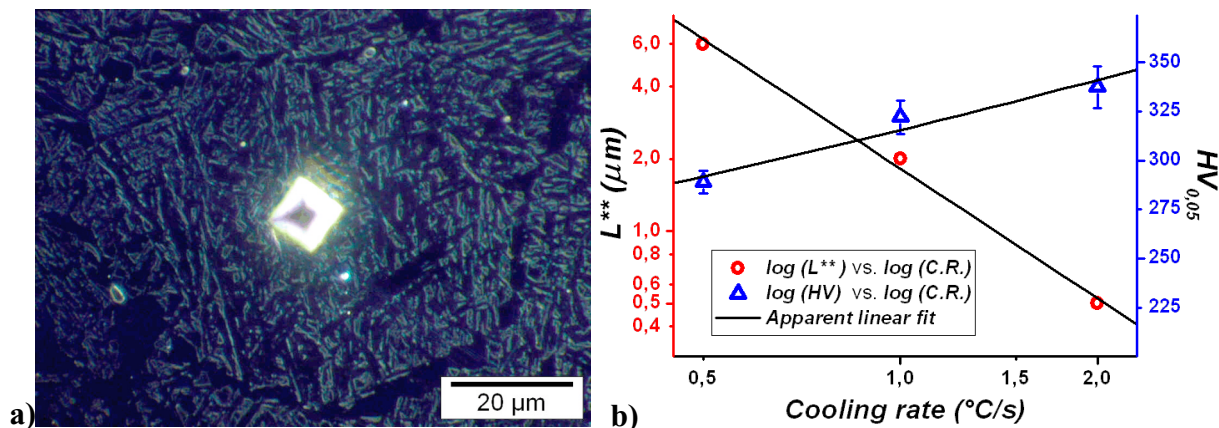


Figure 6. a) Dark field optical image of $HV_{0.05}$ indent imprint. b) Simultaneous log-log plots of cooling rates vs.: lower limit of fractal scale range L^{**} , and AF Vickers hardness $HV_{0.05}$.

Fine precipitation

Figure 7 shows bright field and dark field images of interphase precipitation in proeutectoid ferrite in FA2 steel at 2.0 μ C/s cooling rate. It is common to find interphase precipitation evidences in both proeutectoid ferrite and ferrite lamellas of pearlite in ferrite-pearlite microstructures.

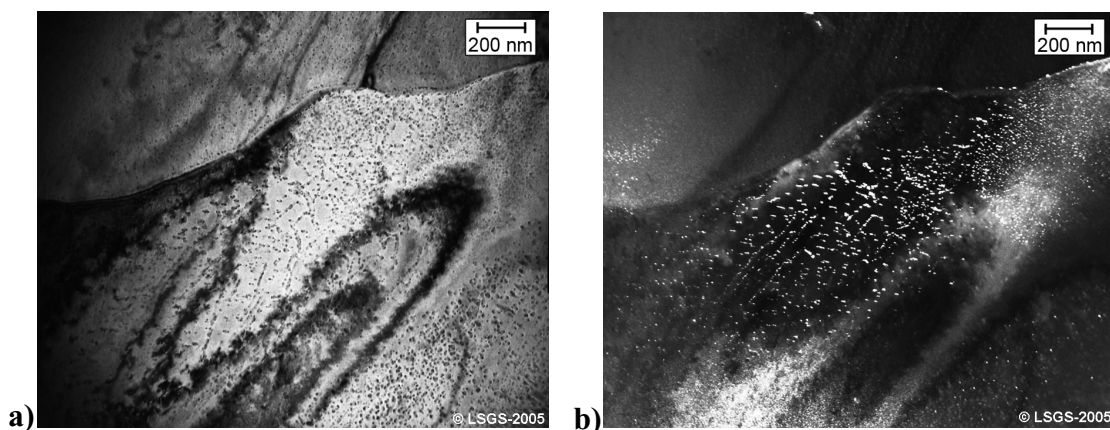


Figure 7. TEM images of interphase precipitation in proeutectoid ferrite in microstructures obtained at 2.0 μ C/s cooling rate. a) Bright field, b) dark field

It is less frequent to find this kind of precipitation in bainite or martensite. Though, some authors have already proposed the VC and/or V(CN) precipitation [23] or Fe-V cluster formation [24] to explain V alloying influence in AF formation. Evidence of these events could not be presented till now, surely because of the lower C content in welded steel and/or highest cooling rates. TEM observation of microstructures treated here has also revealed an interphase precipitation phenomenon inside AF plates (Figure 8).

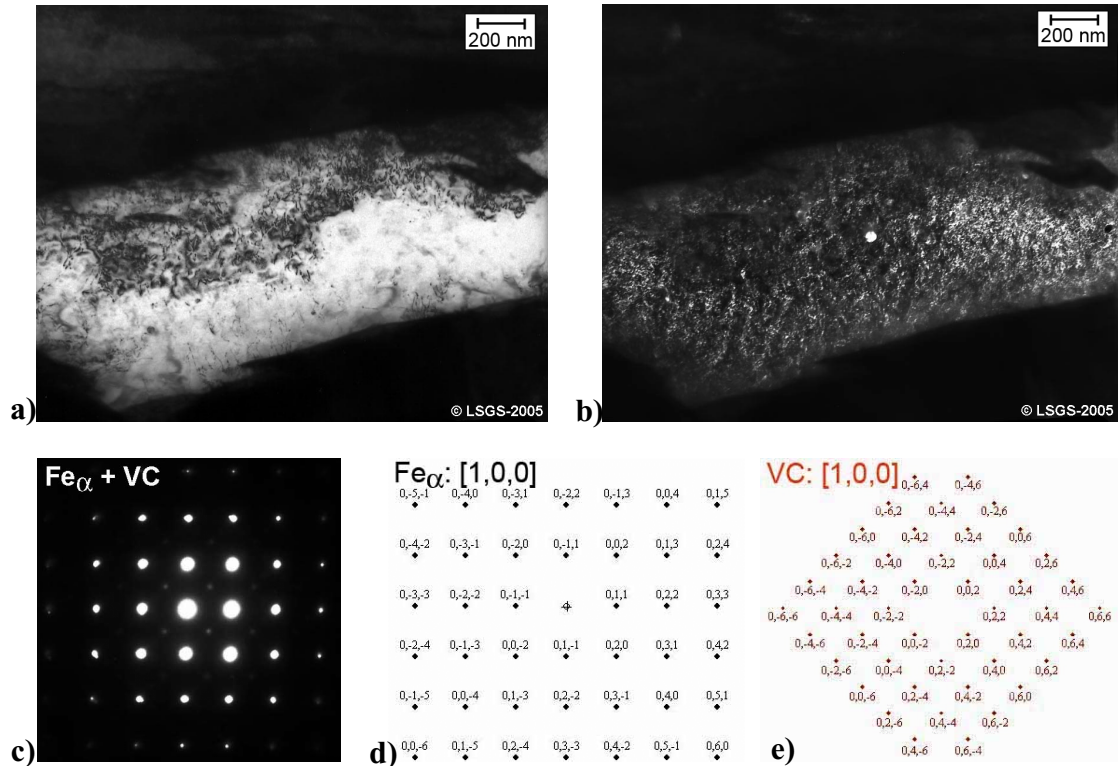


Figure 8. Interphase precipitation inside AF plates. a) Bright field, b) dark field, c) diffraction pattern, d) Fe_{α} indexation, e) VC indexation.

Fine precipitates were identified as VC, presenting a cube-cube crystallographic orientation relationship with ferrite matrix in both proeutectoid ferrite and AF:

$$[001]_{VC} \parallel [001]_{Fe_{\alpha}}, (110)_{VC} \parallel (110)_{Fe_{\alpha}}, (111)_{VC} \parallel (111)_{Fe_{\alpha}}, \quad (1a)$$

$$Fe_{\alpha} : I \frac{4}{m} \bar{3} \frac{2}{m}, \quad G = \frac{4}{m} \bar{3} \frac{2}{m}; \quad VC : F \frac{4}{m} \bar{3} \frac{2}{m}, \quad G_{VC} = \frac{4}{m} \bar{3} \frac{2}{m} \quad (1b)$$

$$Shared \ symmetry \ elements : H^{Fe/VC} = G_{48}^{Fe} \cap G_{48}^{VC} = \frac{4}{m} \bar{3} \frac{2}{m} \quad (1c)$$

$$Variant \ number : n = \frac{48}{48} = 1 \quad (1d)$$

This kind of precipitation, as expected, visibly increases with V content, and it was more significant in proeutectoid ferrite than in AF. Since one of the most probable mechanisms for nucleation of AF is due to the formation of solute-depleted regions [25], it is reasonable to think that the fine precipitation of VC is directly linked with the AF rate increase noted [14].

CONCLUSIONS

Fractal analysis carried on AF microstructures in medium carbon micro-alloyed steel had been evidenced the self similarity and the existence of a fractal dimension D in microstructures obtained by continuous cooling at rates between 0.5 - 2.0 μ C/s. A first step in establishing a relationship between fractal parameters and mechanical properties had been done. Vickers hardness presents an inverse exponential relation with lower fractal scale range limit L^{**} . Fine VC interphase precipitation had been found in TEM observations in

proeutectoid ferrite as well as inside AF ferrite plates. This precipitation could explain the increase in AF rate with vanadium content in medium carbon micro-alloyed steels.

REFERENCES

1. H. K. D. H. Bhadeshia, *Materials Science Forum* Vols. 284-286 (1998) pp. 39-50.
2. H. K. D. H. Bhadeshia, *Bainite in Steels*, Second Edition, 2001, IOM Comm. Ltd.
3. S. S. Babu, H. K. D. H. Bhadeshia, *Materials Transactions, JIM*, Vol. 32, No. 8 (1991) pp. 679-688
4. J-R. Yang, Ph. D. degree thesis, University of Cambridge, (1987).
<http://www.msm.cam.ac.uk/phase-trans/2000/phd.html>
5. J-R. Yang, H. K. D. H. Bhadeshia, *Materials Science and Technology*, Jan. 1989, Vol. 5, pp. 93-97
6. M. A. Linaza, J. L. Romero, J. M. Rodriguez-Ibabe, J. J. Urcola, *Scripta Metallurgica et Materialia*, Vol. 29, (1993), pp. 1217-1222
7. M. Diaz, I. Madariaga, J. M. Rodriguez-Ibabe, I. Gutierrez, *Journal of Constructional Steel Research* (UK), Vol. 46, no. 1-3, pp. 413, Apr.-June 1998.
8. I. Madariaga, I. Gutierrez, *Materials Science Forum* Vols. 284-286 (1998) pp. 419-426.
9. Ming-Chun Zhao, Ke Yang, Fu-Ren Xiao and Yi-Yin Shan, *Materials Science and Engineering A*, Vol. 355, Issues 1-2, 25 August 2003, pp. 126-136.
10. S.K. Dhua, D. Mukerjee, D.S. Sarma, *Metallurgical and Materials Transactions A*, Vol. 34A, Nov. 2003, pp. 2493-2504.
11. S. Das, A. Ghosh, S. Chatterjee, P. Ramachandrarao, *Scandinavian Journal of Metallurgy*, 2004; Vol. 33: pp. 203-210.
12. A. A. B. Sugden, H. K. D. H. Bhadeshia, *Metallurgical Transactions A*, Vol. 20A, September 1989, pp. 1811-1818.
13. J. R. Yang, H. K. D. H. Bhadeshia, *Journal of Materials Science*, 26 (1991) 839-845.
14. R. Villegas, A. Redja mia, L. Marot, M. Confente, L. Marot, M.T. Perrot-Simonetta, *Traitement Thermique* 357 Ao t-Sept. 2004, pp. 29-33.
15. Benoit B. Mandelbrot, *The fractal geometry of nature*, New York: Freeman, (1983).
16. E. Hornbogen, *Prakt. Metallographie*, Vol. 23, (1986) pp. 258-267.
17. H. Takayasu, *Fractals in Physical Sciences*, Manchester University Press, Manchester, New York, (1990)
18. J. M. Li, Li Lu, M. O. Lai, B. Ralph, *Image-Based Fractal Description of Microstructures* Kluwer Academic Publishers, (2003), ISBN:1402075073.
19. B. Skrotzki, *Journal of Materials Science*, Vol. 26 (1991) pp. 1073-1077.
20. N. Jost, E. Hornbogen, *Prakt. Metallographie*, Vol. 25, (1988) pp. 157-173.
21. E. Hornbogen, *Materials Science Forum*, Vol. 56-58 (1990) pp. 131-138.
22. M. Tanaka, *Journal of Material Science*, Vol. 30 (1995) pp. 3668-3673.
23. T. Furuhashi, J. Yamaguchi, N. Sugita, N. Miyamoto, T. Maki. *ISIJ Int*, 2003; Vol. 43: pp. 1630—1639.
24. He K, Edmonds DV. *Mater Sci Technol*, 2002; Vol. 18, pp. 289—96.
25. S. S. Babu, *Current Opinion in Solid State and Materials Science*, Vol. 8, Issues 3-4, June-August 2004, pp. 267-278